DALTON

Control of the co-ordination mode of 1,8-naphthyridine ligated to ruthenium(II) bipyridine complexes

Hiroshi Nakajima,[a] Hirotaka Nagao[b] and Koji Tanaka *,[a]

[a] *Institute for Molecular Science, Department of Structural Molecular Science, The Graduate University for Advanced Studies, Myodaiji, Okazaki 444, Japan*
[b] *Department of Chemistry, Faculty of Science and Technology, Sophia University, 7–1, Kioi-cho, Chiyoda-ku 102, Japan*

The complexes $[Ru(bipy)_2(napy\text{-}N)(MeCN)][PF_6]_2$ **1** and $[Ru(bipy)_2(napy\text{-}N,N')][PF_6]_2$ **2** (bipy = 2,2′-bipyridine, napy = 1,8-naphthyridine) were prepared, and their crystal structures determined by X-ray analysis. The crystal structure of **1** displays an octahedral co-ordination with monodentate napy, acetonitrile and two chelating bipy. Despite the inequivalency of two nitrogens of napy in **1** in the solid state, the ^1H NMR spectra in the aromatic region resemble those of **2** over the range −90 to 60 °C, which implies dynamic behaviour of napy in **1** in solution. Both **1** and **2** were reduced irreversibly at −0.98 V (*vs.* Ag–AgCl) in dimethylformamide at −20 °C, and the process gradually becomes a reversible redox reaction on increasing the temperature to 30 °C. An EPR study revealed that one-electron reduction of **1** takes place in the napy-localized orbital without appreciable increase in electron density on one of the nitrogens of napy. The distinct inequivalence in the charge density between the two nitrogen atoms of singly reduced napy results in stabilization of the *N* rather than *N,N′* co-ordination mode.

In homogeneous catalytic reactions, site opening of catalysts only when reactions take place would be preferable for stabilization of the catalysts, inhibition of side reactions and promotion of product elimination from a reaction centre. To construct such a reaction system the catalysts would be required to have ligands which can adopt different co-ordination modes reversibly with little configurational barrier. It is known that 1,8-naphthyridine (napy) co-ordinates to metals through mono-[1–3] and bi-dentate.[4] In addition, some monodentate napy ligands exhibit bidentate character in solution depending on the temperature owing to rapid site exchange between the two nitrogens.[2,3] Therefore, napy is expected to be a suitable compound for the design of homogeneous catalysts having site-opening and -closing functions. The dynamic behaviour of napy in the complexes $[Ru(bipy)_2(napy\text{-}N)(solv)]^{n+}$ and $[Ru(bipy)_2(napy\text{-}N,N')]^{n+}$ (n = 1 or 2; bipy = 2,2′-bipyridine, solv = solvent) in solution has therefore been investigated.

Experimental

Materials

Tetrabutylammonium tetrafluoroborate was obtained from Nakarai Tesque and recrystallized from methanol. Acetonitrile and ethanol were distilled over CaH_2 before use. All other chemicals were used without further purification. The complex $[Ru(bipy)_2Cl_2]\cdot 2H_2O$ was prepared according to a previously described method.[5]

Preparations

$[Ru(bipy)_2(napy\text{-}N,N')][PF_6]_2$ 2. An ethanol solution (30 cm^3) containing $[Ru(bipy)_2Cl_2]\cdot 2H_2O$ (200 mg) and a 4 molar excess of 1,8-naphthyridine (200 mg) was refluxed for 2 h during which time the solution changed from dark purple to reddish brown. It was then concentrated to *ca.* 3 cm^3 under reduced pressure. Addition of an excess of NH_4PF_6 gave $[Ru(bipy)_2(napy\text{-}N)Cl]PF_6$ together with a small amount of $[Ru(bipy)_2(napy\text{-}N,N')][PF_6]_2$. A 2-methoxyethanol solution (35 cm^3) containing crude $[Ru(bipy)_2(napy)Cl]PF_6$ (100 mg) and $AgPF_6$ (34 mg) was stirred at 90 °C for 2 h under N_2. After cooling to ambient temperature, the solution was filtered over Celite to remove AgCl and then evaporated. Treatment of the product with a chilled aqueous solution of NH_4PF_6 afforded $[Ru(bipy)_2(napy\text{-}N,N')][PF_6]_2$ as a dark red precipitate which was filtered off, washed with diethyl ether, and dried *in vacuo*. The compound was purified by recrystallization from acetone. Yield: *ca.* 70% based upon $[Ru(bipy)_2Cl_2]\cdot 2H_2O$ (Found: C, 40.20; H, 2.70; N, 10.05. Calc. for $C_{28}H_{22}F_{12}N_6P_2Ru$: C, 40.30; H, 2.65; N, 10.10%).

$[Ru(bipy)_2(napy\text{-}N)(MeCN)][PF_6]_2$ 1. Complex **2** (100 mg) was dissolved into acetonitrile (35 cm^3) and stirred for 3 h at room temperature. After evaporation under reduced pressure, the product was treated with an aqueous solution of NH_4PF_6 to afford $[Ru(bipy)_2(napy\text{-}N)(MeCN)][PF_6]_2$ as a yellowish orange precipitate which was filtered off, washed with diethyl ether, and dried *in vacuo*. The compound was purified by recrystallization from acetone–EtOH (7:3 v/v). Yield: *ca.* 85% based upon $[Ru(bipy)_2(napy\text{-}N,N')][PF_6]_2$ (Found: C, 40.55; H, 2.80; N, 11.05. Calc. for $C_{30}H_{25}F_{12}N_7P_2Ru$: C, 41.20; H, 2.90; N, 11.20%).

Physical measurements

Infrared spectra were obtained on a Shimadzu FTIR-8100 spectrophotometer, ^1H NMR spectra on a JEOL EX270 spectrometer (270 MHz) with a temperature controller. Elemental analyses were carried out at the chemical materials centre of the Institute for Molecular Science. Cyclic voltammetric experiments were performed in MeCN or dimethylformamide (dmf) containing 0.1 mol dm^{-3} $NBu^n_4BF_4$ with a Hokuto Denko HA-151 potentiostat/function generator and a Riken Denshi Co. F-35 X-Y recorder. The cell consisted of a glassy carbon working electrode (0.07 cm^2), a platinum-wire auxiliary electrode and an Ag–AgCl reference electrode. The $E_{\frac{1}{2}}$ values reported were determined from the average of the oxidative and reductive peak potentials. Electronic absorption spectra were recorded on a Hewlett-Packard 8452A diode-array spectrophotometer.

Samples for EPR measurements were prepared electrochem-

ically in dmf containing complex **1** (5.0×10^{-3} mol dm^{-3}) and $NBu^n_4BF_4$ (5×10^{-2} mol dm^{-3}) under N_2. The complex was reduced at -1.0 V (*vs.* Ag–AgCl) at a platinum-mesh electrode, and transferred to a capillary with a Teflon tube. The spectra of the samples were recorded at 0 °C with a Bruker ESP 300E spectrometer equipped with a temperature controller.

Crystallography

Single crystals suitable for X-ray analysis were grown by diffusing diethyl ether over ethanol–acetone solutions of complexes **1** and **2**. Data were collected by the ω–2θ scan technique ($6 < 2\theta < 50°$ for **1** and $6 < 2\theta < 55°$ for **2**) on an Enraf-Nonius CAD4-GX21 automated four-circle diffractometer with Mo-Kα radiation (λ 0.7107 Å). The 4992 and 1337 independent reflections for **1** and **2**, respectively, with $I_o > 3\sigma(I_o)$ were used for the structure refinement. All the calculations were carried out on a Silicon Graphics IRIS indigo computer system using TEXSAN.[6] The structures were solved by direct methods and expanded using Fourier techniques. Empirical absorption corrections were made using the program DIFABS[7] resulting in transmission factors ranging from 0.94 to 1.06 and 0.92 to 1.06 for **1** and **2**, respectively. The non-hydrogen atoms except the fluorine atoms of **2** were refined anisotropically, and hydrogen atoms were placed in idealized positions. Refinements were performed using full-matrix least-squares procedures. Since the PF_6 anions of **2** were affected by disorder, two plausible sets of six fluorine atoms were chosen from the Fourier-difference map and refined isotropically.

Complete atomic coordinates, thermal parameters and bond lengths and angles have been deposited at the Cambridge Crystallographic Data Centre. See Instructions for Authors, *J. Chem. Soc., Dalton Trans.*, 1996, Issue 1.

Results and Discussion

Crystal structures of complexes 1 and 2

The napy-*N* ligated complex **1** was easily prepared by concentration of a MeCN solution of the napy-*N*,*N*′ ligated complex **2** (see Experimental section), although there had been controversy concerning the possibility of dechelation of the napy ligand in **2** in dilute MeCN solution.[8] Successful recrystallization of **1** from EtOH–Me_2CO suggests the stability of **1** in solution without the presence of excessive MeCN.

Table 1 Crystal data for complexes **1** and **2**

Complex	**1**	**2**
Colour	Reddish yellow	Dark red
Formula	$C_{30}H_{25}F_{12}N_7P_2Ru$	$C_{28}H_{22}F_{12}N_6P_2Ru$
M	874.57	833.52
Crystal system	Triclinic	Orthorhombic
Space group	$P\bar{1}$ (no. 2)	*Pbcn* (no. 60)
a/Å	13.389(5)	12.514(2)
b/Å	13.590(2)	15.077(3)
c/Å	10.577(2)	17.489(4)
α/°	104.19(2)	
β/°	109.47(2)	
γ/°	76.48(2)	
U/Å^3	1734.6(8)	3299.7(10)
Z	2	4
D_c/g cm^{-3}	1.67	1.68
F(000)	872	1688
Crystal dimensions/mm	0.2 × 0.2 × 0.4	0.2 × 0.4 × 0.5
μ(Mo-Kα)/cm^{-1}	6.43	6.71
No. unique data	6447	4224
No. observed data	4992	1337
Final *R*, *R*′	0.058, 0.069	0.070, 0.058

[a] $R = \Sigma||F_o| - |F_c||/\Sigma|F_o|$, $R' = [\Sigma w(|F_o| - |F_c|)^2/\Sigma wF_o^2]^{\frac{1}{2}}$, $w = 1/\sigma^2(F_o)$.

Crystallographic data and selected bond distances, angles and dihedral angles for **1** are given in Tables 1 and 2, respectively. An ORTEP view with the atomic numbering scheme is shown in Fig. 1. The ruthenium atom is octahedrally co-ordinated by two nitrogens of MeCN and napy ligands in *cis* positions, and four nitrogen atoms of two bipy ligands. The Ru–N(1) bond distance of 2.14 Å is close to that of Mn–napy-*N* complexes (2.11 Å).[2] The almost linear N(1)–Ru–N(3) bond angle (176.7°) and long Ru • • • N(2) distance (3.24 Å) compared with the sum of the covalent radii of Ru^{II} (1.25 Å) and N(sp^2) (0.68 Å) reveals little interaction between Ru and N(2) of napy. The aromatic ring containing N(2) is located the space between the axial and equatorial bipy ligands, and the torsion angles N(4)–Ru–N(1)–C(8) and N(6)–Ru–N(1)–C(8) are 49.6 and 49.1°, respectively. The Ru–NCMe bond distance of 2.02 Å is similar to those of $[Ru(bipy)_2(MeCN)_2]^{2+}$ (2.03 Å)[10] suggesting that this bond in **1** is not largely affected by the napy ligand in the crystal.

Fig. 2 shows an ORTEP view of complex **2** with the atomic numbering scheme. The crystallographic data and selected bond distances, angles and dihedral angles are given in Tables 1 and 3, respectively. A small chelate bite (62.8°) is observed for napy-*N*,*N*′, and probably due to this distortion the bond angle N(1)–C(5)–N(1′) is somewhat strained (109°) compared to that of N(2)–C(8)–N(1) in **1** (116.1°). The Ru–N(1) (2.11 Å) distance is similar to that in **1** (2.14 Å) suggesting that the bond strength between the ruthenium and napy is not increased by chelation

Table 2 Selected bond distances (Å), angles (°) and dihedral angles (°) of complex **1**

Ru–N(1)	2.137(6)	Ru–N(6)	2.058(5)
Ru–N(3)	2.047(6)	Ru–N(7)	2.023(5)
Ru–N(4)	2.069(5)	N(7)–C(29)	1.115(9)
Ru–N(5)	2.063(5)	C(29)–C(30)	1.47(1)
N(3)–Ru–N(4)	78.2(2)	N(5)–Ru–N(6)	78.4(2)
N(1)–Ru–N(3)	176.7(2)	N(6)–Ru–N(7)	174.5(2)
N(5)–Ru–N(4)	173.5(3)	Ru–N(7)–C(29)	172.7(7)
N(7)–C(29)–C(30)	177(1)	N(2)–C(8)–N(1)	116.1(7)
N(4)–Ru–N(1)–C(8)	49.6(5)	N(6)–Ru–N(1)–C(8)	49.1(5)
N(7)–Ru–N(1)–C(1)	43.1(5)	N(5)–Ru–N(1)–C(1)	53.3(5)

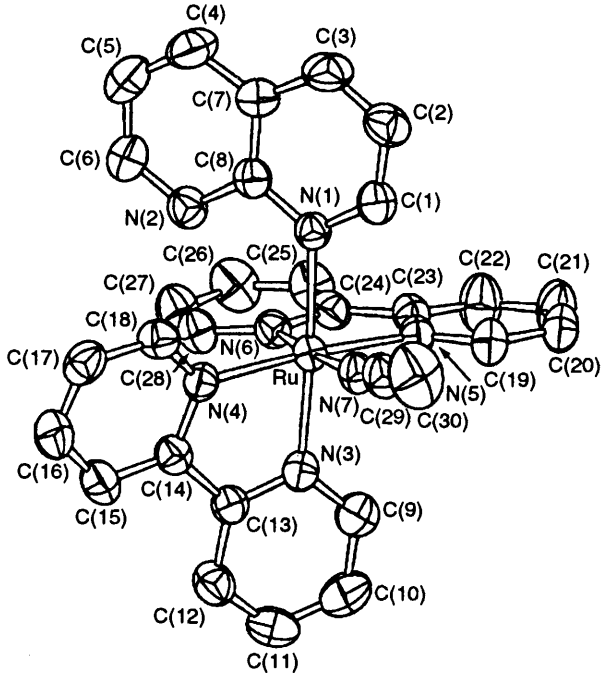

Fig. 1 An ORTEP view of complex **1** with the atom numbering system. The atom positions are indicated with 50% probability ellipsoids

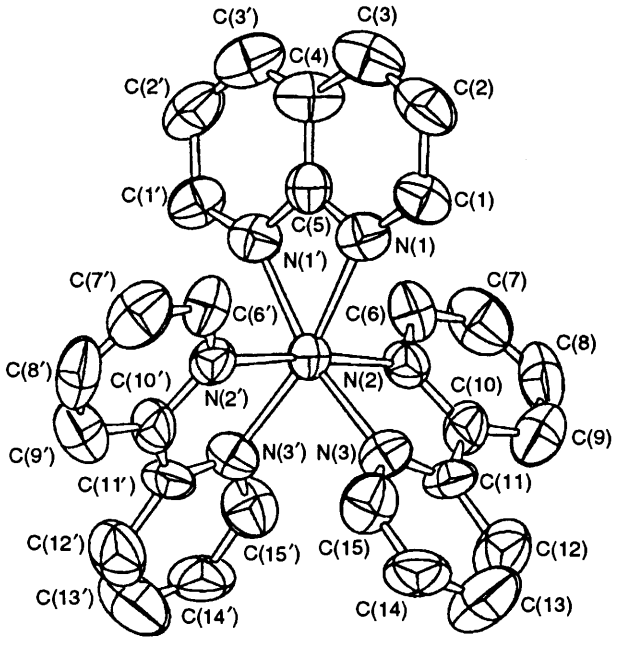

Fig. 2 An ORTEP view of complex **2** with the atom numbering system. The atom positions are indicated with 50% probability ellipsoids

Table 3 Selected bond distances (Å), angles (°) and dihedral angles (°) of complex **2**

Ru–N(1)	2.11(1)	Ru–N(3)	2.05(9)
Ru–N(2)	2.09(9)		
N(1)–Ru–N(1′)	62.8(6)	N(2)–Ru–N(3)	78.2(4)
N(1)–C(5)–N(1′)	109(2)	N(2)–Ru–N(3′)	97.3(4)
N(2)–Ru–N(2′)	174.0(6)		
N(3)–Ru–N(1)–C(5)	173.9(5)	N(1)–C(5)–C(4)–C(3)	1.8(9)
N(1′)–Ru–N(2)–C(6)	7(1)	N(2′)–Ru–N(3)–C(15)	1(1)

of napy. A two-fold axis passes through Ru, C(4) and C(5), and the symmetry in the crystal structure is possibly retained in solution since the ^{1}H NMR spectrum of **2** showed magnetic equivalence of the two rings of the napy ligand in the range −90 to 60 °C (see below).

Electronic absorption spectra

The electronic absorption spectra of a large number of $[Ru(bipy)_2L_2]^{2+}$ (L = amine) complexes are characterized by strong π–π* absorption in the UV region and a metal-to-ligand charge-transfer m.l.c.t. bands around 450 nm.[11,12c] The absorption maxima of **1** and **2** in CH_2Cl_2 are identical in the π–π* region, and the m.l.c.t. bands are observed at 448 and 450 nm, respectively. As expected from the smooth conversion of **2** into **1** in MeCN, both complexes showed the same electronic absorption spectra in MeCN[8] (Table 4). The blue shift of the m.l.c.t. band (λ_{max} = 434 nm) in MeCN compared with that in CH_2Cl_2 is characteristic of ligation of MeCN to ruthenium poly(pyridyl) complexes.[13] The slight difference in the m.l.c.t. bands of **1** and **2** in CH_2Cl_2, therefore, suggests the presence of **1** in CH_2Cl_2 even in the absence of an excess of MeCN although the interaction between the ruthenium and the MeCN ligand is weak.

Proton NMR spectra

Fig. 3(*a*) shows the NMR spectrum of complex **2** in CD_2Cl_2 at room temperature. The proton signals of the two bipy and one napy ligand were assigned by two-dimensional NMR spectroscopy. The protons of napy were identified by

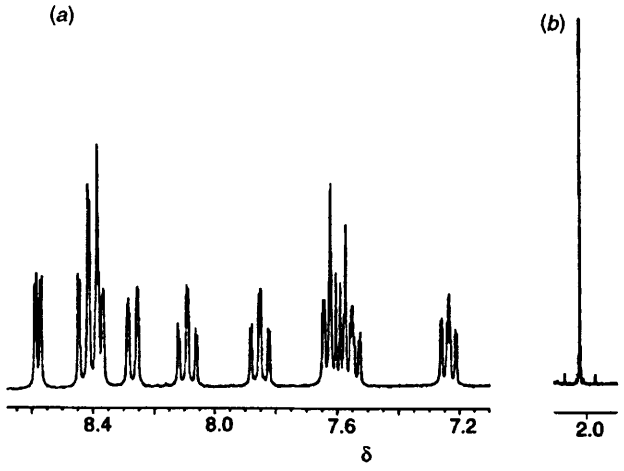

Fig. 3 Proton NMR spectra (270 MHz) in CD_2Cl_2 at room temperature; (*a*) the aromatic region of complex **2** and (*b*) the methyl signal of the MeCN ligand of **1**

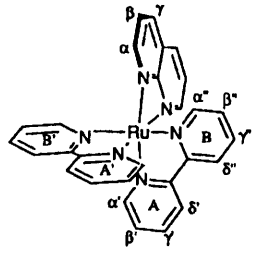

A

Table 4 Electronic absorption spectral data for complexes **1** and **2** at 25 °C

Complex	Solvent	λ_{max}/nm	10^{-4} ε/dm^3 mol^{-1} cm^{-1}
1	CH_2Cl_2	248	2.16
		256	2.43
		288	7.43
		448	1.30
2	CH_2Cl_2	248	2.20
		256	2.41
		288	7.22
		450	1.24
1	MeCN	243	2.90
2		254	2.74
		288	5.93
		434	1.50

correlation (COSY) spectroscopy for H_α, H_β and H_γ (δ 8.58, 7.59 and 8.40, respectively) (structure **A**). As expected from the crystal structure, the ^{1}H NMR signals of napy in **2** show a magnetic equivalency of the two aromatic rings. Similarly, a magnetic equivalency of the A and A′ and of B and B′ ring protons of the bipy ligands was evidenced by COSY for two sets of pyridyl protons ($H_{\alpha'}$, $H_{\beta'}$, $H_{\gamma'}$ and $H_{\beta'}$, $H_{\gamma'}$, $H_{\delta'}$) and ($H_{\alpha''}$, $H_{\beta''}$, $H_{\gamma''}$ and $H_{\beta''}$, $H_{\gamma''}$, $H_{\delta''}$). The positions of $H_{\alpha'}$ and $H_{\alpha''}$ were deduced from ring current effects based on the assignment of the aromatic protons of $[Ru(bipy)_3]^{2+}$;[14] the α′-proton located below the A′ ring would be shielded by a ring current from the A′ ring resulting in a higher field shift of its signal (δ 7.63) than that of the α″-proton (δ 8.38) which is placed outside the aromatic ring of napy.

The ^{1}H NMR spectrum of complex **1** in CD_2Cl_2 is similar to that of **2** except for the methyl proton of the MeCN ligand at δ 2.11 [Fig. 3(*b*)]. On the basis of the chemical shifts of free MeCN (δ 1.97) and $[Ru(bipy)_2L(MeCN)]^{2+}$ (δ *ca.* 2.5 for L =

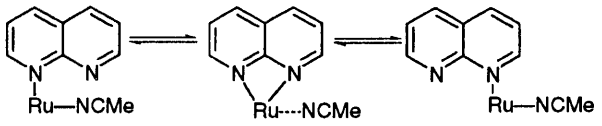

Scheme 1

quinoline,[12a] CO and MeCN*), the appearance of the signal of ligated MeCN at δ 2.11 implies a partial dissociation of MeCN from **1** in CD_2Cl_2. The resemblance of the signals of **1** and **2** in the aromatic region and the equivalency of the two rings of napy, therefore, suggest a rapid isomerization between **1** and **2** accompanied by reversible dissociation of MeCN (Scheme 1). Some metal complexes of napy-*N* show a similar isomerization through bidentate napy, and the fluxionality in their NMR spectra is usually frozen below −90 °C.[2,3] On the other hand, the NMR spectra of **1** was essentially unchanged on lowering the temperature to −90 °C except for a slight lower-field shift (0.06 ppm). Furthermore, raising the temperature to 60 °C resulted in no clear change in the spectrum in [$^2H_6$]dmf. Thus, the limiting spectra of **1** with a napy-*N* ligand was not detected in the present study.

Electrochemical behaviour

Fig. 4(*a*) shows representative cyclic voltammograms of complexes **1** and **2** in dmf. Similar results were obtained in CH_2Cl_2 and acetone solutions. As expected from the equilibrium between **1** and **2** in solution, the voltammograms resemble each other in the range −20 to 30 °C and display three successive one-electron redox couples (the third couple could not be observed in CH_2Cl_2 owing to solvent decomposition at potentials more negative than −1.7V). In contrast to the lack of temperature dependence of the NMR spectra of **1**, the first redox couple largely depends on the temperature. A large peak separation of the first anodic and cathodic waves ($E_{p,a}$ = −0.22 and $E_{p,c}$ = −0.96 V *vs.* Ag–AgCl, respectively) of 640 mV at −20 °C continuously decreases on increasing the temperature and finally becomes 60 mV at 30 °C [Fig. 4(*a*)]. The redox potentials of the second and third reversible couples at $E_{\frac{1}{2}}$ = −1.40 and −1.68 V are almost independent of temperature despite the drastic change in the first redox couple. In addition, the NMR spectrum of **1** in dmf was not changed at all even after one-electron reduction of the complex at −1.1 V and subsequent oxidation at 0 V. Thus, **1** does not undergo a degradation reaction after a one-electron reduction–oxidation cycle. The cyclic voltammograms of both complexes **1** and **2** in MeCN also show a temperature-dependent redox couple and two temperature-independent reversible redox couples. A cathodic wave at $E_{p,c}$ = −1.40 V (*vs.* Ag–AgCl) coupled with a weak anodic wave at $E_{p,a}$ = −0.58 V and successive reversible redox waves at $E_{\frac{1}{2}}$ = −1.50 V are observed at 0 °C [solid line of Fig. 4(*b*)].† The anodic and cathodic waves at −0.58 and −1.40 V shift to more negative and positive potentials, respectively, on raising the temperature, occurring at −1.02 and −1.31 V, respectively, at 50 °C. Thus, the reversibility of the first redox couple is gradually improved with increasing temperature, although the relatively large peak separation between the cathodic and anodic waves (290 mV) still remains at 50 °C. (One-electron reduction of **1** at > 50 °C resulted in its decomposition.) The increase in the reversibility of the $\mathbf{1}^{2+/+}$ couple at higher temperature (Fig. 4) reasonably excludes the possibility of dissociation of any ligands from the 2+ and 1+ species since metal–ligand bonds would strengthen with decreasing temperature.

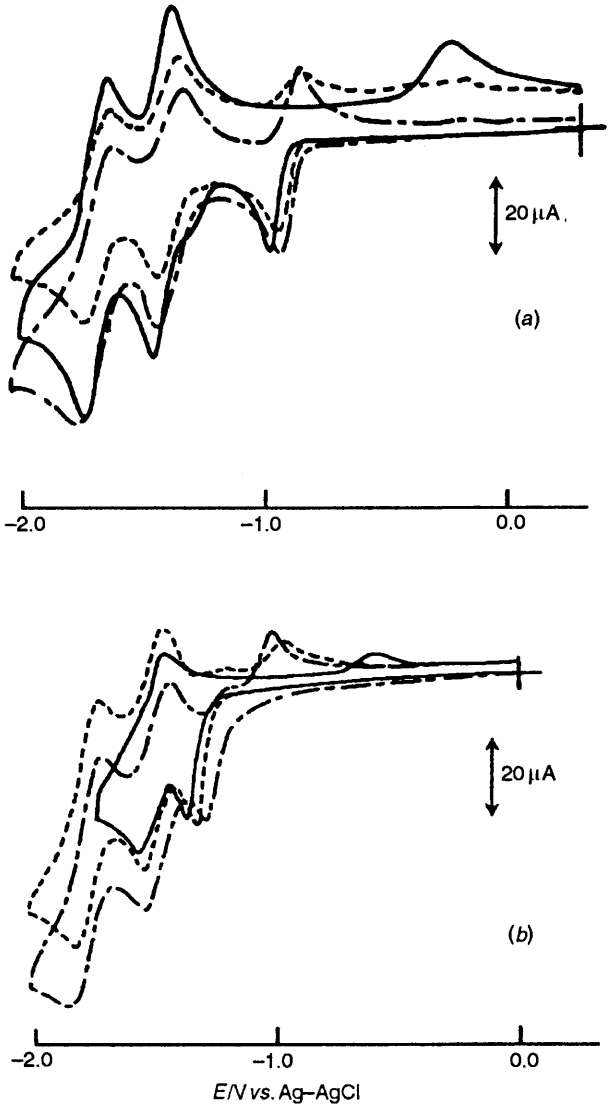

Fig. 4 Representative cyclic voltammograms of complex **1**, (*a*) in dmf at −20 (——), 5 (– – –) and 30 °C (— — —), in (*b*) MeCN at 0 (——), 25 (– – –) and 50 °C (— — —); dE/dt = 100 mV s^{-1}. Complex **2** shows similar spectra under the same conditions

EPR spectra

The EPR spectrum of the one-electron reduced species of complex **1** is expected to afford fundamental information on the unusual temperature dependence of the 2+/1+ redox process. A red solution obtained on controlled-potential electrolysis of **1** at −1.1 V in dmf gave a well resolved hyperfine structure due to the one-electron reduced species [Fig. 5(*a*)]. (The corresponding spectrum from **2** was almost identical.) A computer simulation using a^H, a^N and *g* values listed in Table 5 gave excellent agreement with the observed EPR spectrum as shown in Fig. 5(*b*). The *g* value of 2.0046 typical of organic radical anions and the hyperfine couplings with six protons and one nitrogen (Table 5) indicate that the electron introduced into **1** is accommodated mainly in a localized molecular orbital on napy rather than the bipy ligands or the ruthenium. The most striking point in Table 5 is the lack of a hyperfine coupling with one of the nitrogens of napy. It has been reported that one-electron reduction of $[Ru(bipy)_2(bpz)]^{2+}$ (bpz = bipyrazine) enhances the electron density on the co-ordinated nitrogens and on the *ortho* carbons of bpz, and the contribution to the electron population is minimal for its non-bonded nitrogen atoms.[15] On the basis of the fact that the equilibrium between **1** and **2** in

* The complexes $[Ru(bipy)_2L(MeCN)]^{2+}$ (L = CO[12b] or MeCN[12c]) were prepared using previously described methods and the ^1H NMR measurements were performed in CD_2Cl_2 at room temperature.

† Detection of the reversible redox couple at $E_{\frac{1}{2}}$ = −1.77 V was hampered in MeCN at −5 °C due to adsorption of the three-electron reduced species of **1** on the surface of the glassy carbon electrode.

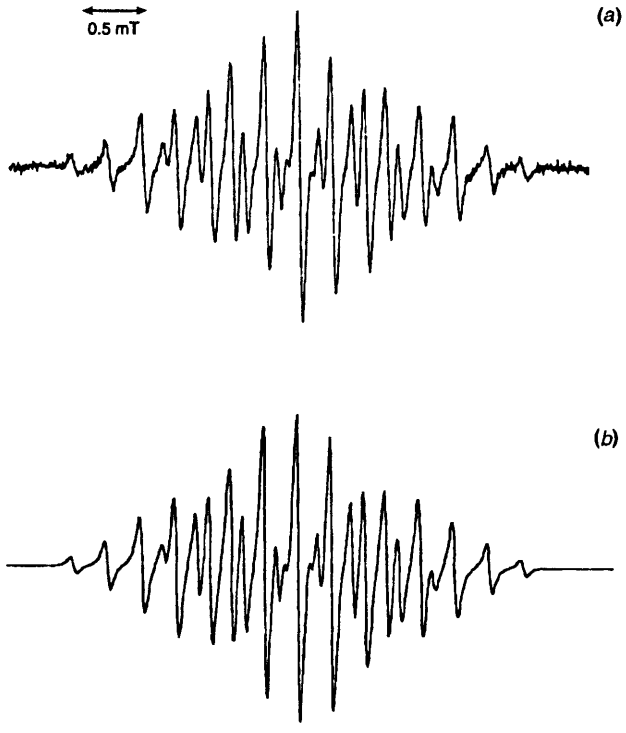

Fig. 5 First-derivative EPR spectrum of singly reduced complex **1** in dmf with $NBu^n_4BF_4$ (5×10^{-2} mol dm^{-3}) at 0 °C (*a*) and computer-simulated spectrum using coupling constants given in Table 5(*b*)

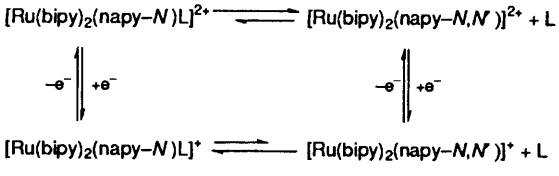

Scheme 2 L = solvent

Table 5 The EPR parameters of one-electron-reduced complex **1**

a^H/mT	Multiplicity	a^N/mT	Multiplicity	*g*
0.70	2	0.27	1	2.0046
0.53	2	≈0	1	
0.27	2			

dmf shifts towards the latter, the significantly different electron density on the two nitrogen atoms of napy (Table 5) may be associated with destabilization of the napy-*N*,*N*′ co-ordination mode upon introduction of one electron into a localized molecular orbital of napy. The single-electron reduction of **1** and **2** would, therefore, result in an asymmetric co-ordination of napy and maybe to its dechelation. If $[Ru(bipy)_2(napy\text{-}N)(solv)]^+$ also exists as an equilibrium mixture with **2** similar to the equilibrium between **1** and **2**, the unusual temperature dependence of the 2+/1+ redox couple of **2** in (Fig. 4) is reasonably explained by Scheme 2. The equilibrium between complexes $\mathbf{1}^{2+}$ and $\mathbf{2}^{2+}$ shifts towards the latter, while $\mathbf{1}^+$ is the main species in their reduced forms. One-electron reduction of **2**, therefore, is accompanied by a change in the co-ordination mode from napy-*N*,*N*′ to -*N*. On the other hand, loss of solvent from $\mathbf{1}^+$ at higher temperatures would shift the equilibrium from napy-*N* to -*N*,*N*′ ligated $\mathbf{2}^+$. The appearance of the reversible $\mathbf{2}^{2+/+}$ redox couple in dmf at 30 °C [a broken line in Fig. 4(*a*)], therefore indicates that $\mathbf{2}^+$ is more stable than $\mathbf{1}^+$ at that temperature. The less reversibile nature of the $\mathbf{2}^{2+/+}$ redox couple in MeCN than that in dmf, CH_2Cl_2 and acetone [Fig. 4(*b*)] reflects the thermal stability of MeCN ligated to $\mathbf{1}^+$ compared with that of dmf, CH_2Cl_2 and acetone. It should be noted that the two co-ordination modes of napy hardly affects the two reversible redox couples at −1.50 and −1.77 V in the cyclic voltammograms of **1** and **2**. This observation also indicates that the $\mathbf{2}^{2+/+}$ redox reactions essentially take place at a localized napy ligand.

Conclusion

The napy ligand on $\mathbf{1}^{n+}$ and $\mathbf{2}^{n+}$ (n = 1 and 2) electrochemically exhibits a dynamic change in co-ordination mode between *N* and *N*,*N*′ and the population of each mode is controlled by both the temperature and solvent affinity towards ruthenium. It should be stressed that the *N* mode becomes predominant in the reduced form (the activated form) of $\mathbf{1}^{2+}$ and $\mathbf{2}^{2+}$ without the dissociation of the napy ligand.

Acknowledgements

We thank Professor S. Fukuzumi, Osaka University for assistance in the EPR simulation. This work is partially supported by Fellowships of the Japan Society for Promotion of Science for Japanese Junior Scientists and a Grant-in-Aid for Scientific Research from the Ministry of Education of Japan.

References

1 M.-J. Bermejo, B. Martinez and J. Vinaixa, *J. Organomet. Chem.*, 1986, **304**, 207; E. L. Enwall and K. Emerson, *Acta Crystallogr., Sect. B*, 1979, **35**, 2562; G. W. Bushnell, K. R. Dixon and M. A. Khan, *Can. J. Chem.*, 1978, **56**, 450.
2 K. R. Dixon, D. T. Eadie and S. R. Stobart, *Inorg. Chem.*, 1982, **21**, 4318; K. R. Dixon, *Inorg. Chem.*, 1977, **16**, 2618; H. Schmidbaur and K. C. Dash, *J. Am. Chem. Soc.*, 1973, **95**, 4855.
3 M.-J. Bermejo, J.-I. Ruiz, X. Solans and J. Vinaixa, *J. Organomet. Chem.*, 1993, **463**, 143; *Inorg. Chem.*, 1988, **27**, 4385; S.-K. Kang, T. A. Albright and C. Mealli, *Inorg. Chem.*, 1987, **26**, 3158.
4 M. Munakata, M. Maekata, S. Kitagawa, M. Adachi and H. Masuda, *Inorg. Chim. Acta*, 1990, **167**, 181; H. Aghabozorg, R. C. Palenik and G. J. Palenik, *Inorg. Chem.*, 1985, **24**, 4214; A. Tiripicchio, M. T. Camellini, R. Usón, L. A. Oro, M. A. Ciriano and F. Viguri, *J. Chem. Soc., Dalton Trans.*, 1984, 125; C. Mealli and F. Zanobini, *J. Chem. Soc., Chem. Commun.*, 1982, 97; A. L. Balch and R. D. Cooper, *J. Organomet. Chem.*, 1979, **169**, 9; D. Gatteschi, C. Mealli and L. Sacconi, *Inorg. Chem.*, 1976, **15**, 2775; *J. Am. Chem. Soc.*, 1973, **95**, 2737; J. C. Dewan, D. J. Kepert and A. H. White, *J. Chem. Soc., Dalton Trans.*, 1975, 492; L. Luigi, C. Mealli and D. Gatteschi, *Inorg. Chem.*, 1974, **13**, 1985; K. Emerson, A. Emad, R. W. Brookes and R. L. Martin, *Inorg. Chem.*, 1973, **12**, 978; A. Clearfield, P. Singh and I. Bernal, *Chem. Commun.*, 1970, 389.
5 B. P. Sullivan, O. J. Salmon and T. J. Meyer, *Inorg. Chem.*, 1978, **17**, 3334.
6 TEXSAN-TEXRAY Structure Analysis Package, Molecular Structure Corporation, Houston, TX, 1985.
7 DIFABS, N. G. Walker and D. Stuart, *Acta Crystallogr., Sect. A*, 1983, **39**, 158.
8 R. J. Staniewicz, R. F. Sympson and D. G. Hendricker, *Inorg. Chem.*, 1977, **16**, 2166.
9 C. K. Johnson, ORTEP, Report ORNL- 5138, Oak Ridge National Laboratory, Oak Ridge, TN, 1976.
10 M. J. Heeg, R. Kroerer and E. Deutsch, *Acta Crystallogr., Sect. C*, **41**, 684.
11 G. M. Brown, T. R. Weaver, F. R. Keene and T. J. Meyer, *Inorg. Chem.*, 1976, **15**, 190; F. R. Keene, D. J. Salmon and T. J. Meyer, *J. Am. Chem. Soc.*, 1976, **98**, 1884.
12 (*a*) H. Nakajima, H. Nagao and K. Tanaka, unpublished work; (*b*) J. M. Kelly, C. M. ÓConnell and J. G. Vos, *J. Chem. Soc., Dalton Trans.*, 1986, 253; (*c*) G. M. Brown, R. W. Calahan and T. J. Meyer, *Inorg. Chem.*, 1975, **14**, 1915.
13 R. J. Staniewicz and D. G. Hendricker, *J. Am. Chem. Soc.*, 1977, **99**, 6581; G. M. Brown, R. W. Callahan and T. J. Meyer, *Inorg. Chem.*, 1975, **14**, 1915.
14 F. E. Lytle, L. M. Petrosky and L. R. Carlson, *Anal. Chim. Acta*, 1971, **57**, 239.
15 J. N. Gen, M. K. Dearmand and K. W. Hanck, *J. Phys. Chem.*, 1987, **91**, 251.

Received 5th September 1995; *Paper* 5/05867H